Available online at www.sciencedirect.com
ScienceDirect
Journal of Molecular Graphics and Modelling 25 (2007) 731–739
Journal of Molecular Graphics and Modelling
www.elsevier.com/locate/JMGM

Classification of α-cyclodextrins inclusion complexes into Type 1 and Type 2: A prelude to log *K* prediction

Giulia Caron *, Giuseppe Ermondi

Dipartimento di Scienza e Tecnologia del Farmaco, Università di Torino, Via P. Giuria 9, I- 10125 Torino, Italy

Received 14 April 2006; received in revised form 7 June 2006; accepted 12 June 2006
Available online 17 June 2006

Abstract

Molecular Interaction Fields (MIFs) were used in combination with a small number of geometrical descriptors to separate nine α-CD complexes into Type 1 and Type 2, two classes, respectively, containing complexes having high log *K* and low log *K* values (stoichiometry of 1:1). Calculations were performed on the crystallographic conformations of α-CDs after their separation from the ligand and without minimization. The results show that the computational strategy adopted is able to distinguish Type 1 from Type 2 complexes and that it can be applied to all CD families.

Keywords: α-Cyclodextrin; Inclusion complexes; CSD; *In silico*; MIF; Polarity; Hydrophobicity; Type 1 complex; Type 2 complex

1. Introduction

In the field of drug discovery, most failed compounds have problems associated with their Absorption, Distribution, Metabolism, Excretion, or Toxicity (ADME-Tox) profiles [1]. Virtual, or *in silico*, ADME-Tox prediction is used to evaluate compounds even before they are synthesized, in order to eliminate poor drug candidates early in the drug discovery cycle.

For oral administration, drugs must dissolve and be sufficiently absorbed through the gastrointestinal (GI) tract. Retrospective studies have shown clearly that >40% of drug failures during development are due to poor dissolution and permeability [2]. The FDA (Food and Drug Administration) together with other regulatory organizations has drawn up a Biopharmaceutical Classification System (BCS) [3,4] dividing drugs into four classes on the basis of their solubility and permeability (Type I = high solubility and high permeability, Type II = low solubility and high permeability, Type III = high solubility and low permeability and Type IV = low solubility and low permeability).

Molecular host–guest-based systems are strategies enabling Type II molecules to behave like Type I molecules, with a resulting increase in their oral bioavailability [5]. A widely used host family is the cyclodextrins (CDs), which are cyclic oligosaccharides composed of 6, 7 or 8 dextrose units (α-, β-, and γ-CDs, respectively) joined through 1–4 bonds [6,7] (Fig. 1A). Because of their structural features, CDs tend to form inclusion complexes that improve the solubility of poorly water-soluble compounds [8,9].

For characterization and formulation purposes, CD inclusion complexes must be differentiated from aggregates, but it may also be very important to separate them into two classes, Type 1 and Type 2. According to Muraoka et al. [10] ligands that enter deeply into the CD cavity generate Type 1 complexes, whereas those that only enter shallowly into the cavity generate Type 2 complexes. The relevance of this classification is that each complex class is related to the log *K* (*K* = the stability constant) values, and thus subdivision of compounds into Type 1 and Type 2 may be expected to match log *K* prediction (stoichiometry of 1:1).

In this study, after a preliminary analysis on the CSD database, nine complexes were selected (the corresponding ligands are reported in Fig. 1B) that are stored both as complexes and as single components (ligand and α-CD). The α-CD structures alone were submitted to calculations, to obtain geometrical and physicochemical descriptors that can separate Type 1 from Type 2 complexes. Taken together, the computational results stress the possibility of predicting log *K* for CDs by using *ad hoc* computational tools [11,12].

* Corresponding author. Tel.: +39 0116707282; fax: +39 0116707687.
E-mail address: giulia.caron@unito.it (G. Caron).

1093-3263/$ – see front matter
doi:10.1016/j.jmgm.2006.06.003

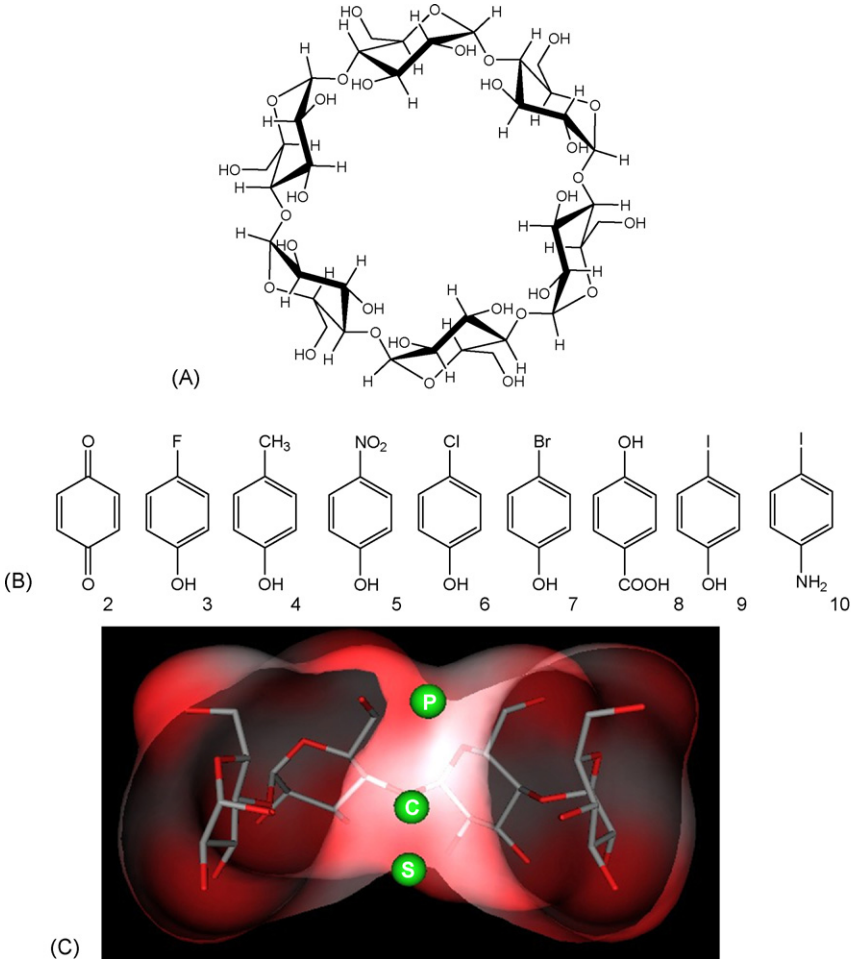

Fig. 1. (A) 2D chemical structures of α-CD (**1**). (B) 2D chemical structures of the ligands forming inclusion complexes with α-CDs and discussed in the text (hydroquinone (**2**), 4-fluorophenol (**3**), 4-methylphenol (**4**), 4-nitrophenol (**5**), 4-chlorophenol (**6**), 4-bromophenol (**7**), 4-hydroxybenzoic acid (**8**), 4-iodophenol (**9**) and 4-iodoaniline (**10**)). (C) The centroids used to define geometrical descriptors employed to characterize α-CD: P is due to the 6 oxygens of the primary face, C to the 6 oxygens joining dextrose units, and S to the 12 oxygens of the secondary face. The Connolly surface is also shown for better visualization of the centroids.

2. Methodology

2.1. α-CD structures retrieved from the Cambridge Structural Database (CSD)

The α-cyclodextrin moiety was used as query to retrieve structures from the Cambridge Structural Database (CSD, Version 5.26; data updates May 2006). The data were checked with mercury [13] to eliminate hits for which no structure was reported, and 31 complexes and 5 structures relating to the α-CD alone were retained. For all α-CDs, three centroids (P, C and S see Section 2.3) were defined and the three corresponding distances (PS, PC and SC) were monitored using MOE [14] (see below for a discussion of the disordered positions of some primary hydroxyl groups).

Among the 36 compounds, 10 were selected to submit to calculations: α-CD alone (code CHXAMH02), the complexes of α-CD with hydroquinone (code PUPTEZ), 4-fluorophenol (code JUMYOF), 4-methylphenol (code WEXLEQ), 4-nitrophenol (code ACDPNP), 4-chlorophenol (code WEXKOZ), 4-bromophenol (code MESYEO), 4-hydroxybenzoic acid (code ACDHBA), 4-iodophenol (code CHAIPL), and with 4-iodoaniline (code CDEXIA01). These 10 compounds were saved in the Tripos mol2 format (necessary for subsequent calculations) and read in MOE [14] to carefully check the coordinates, delete co-crystallized water molecules, separate the α-CD from the ligand and add hydrogen atoms when necessary.

For α-CD as such (=obtained from CHXAMH02) two conformations were stored: **1a**, which was not minimized, and **1b**, which was minimized under MMFF94x in GB-SA conditions [15–17].

For α-CD alone, the following codes were adopted: α-CD separated from hydroquinone = **1d**, from 4-fluorophenol = **1e**, from 4-methylphenol = **1f**, from 4-nitrophenol = **1g**, from 4-chlorophenol = **1h**, from 4-bromophenol = **1i**, from 4-hydroxybenzoic acid = **1j**, from 4-iodophenol = **1k** and from 4-iodoaniline = **1l**.

All selected α-CDs but one (**1e**) have one primary hydroxyl group disordered over two positions. For **1l** this hydroxyl group is missing, whereas in the remaining α-CDs the corresponding oxygen is disordered over two positions with different

Table 1
Distances (in Å) discussed in this study

No.	Ligand	PS	PC	SC	SL	Complex type[a]
1a		4.99	3.15	1.85	–	–
1b		5.21	2.90	2.32	–	–
1c		5.68	3.33	2.37	–	–
1d	Hydroquinone	5.23	3.26	1.98	−0.64	2
1e	4-Fluorophenol	5.21	3.26	1.96	−0.66	2
1f	4-Methylphenol	5.24	3.25	1.99	−0.95	2
1g	4-Nitrophenol	5.08	2.97	2.13	+0.80	1
1h	4-Chlorophenol	4.96	2.82	2.14	+0.79	1
1i	4-Bromophenol	4.97	2.83	2.14	+0.79	1
1j	4-Hydroxybenzoic acid	4.96	2.80	2.16	+0.87	1
1k	4-Iodophenol	5.00	2.85	2.33	+0.52	1
1l	4-Iodoaniline	4.96	2.83	2.13	+0.78	1

P is the centroid due to the 6 oxygen atoms of the primary face, C is the centroid due to the 6 glycosidic oxygen atoms, S is the centroid due to the 12 oxygen atoms of the secondary face and L is the centroid of the aromatic portion of the ligand.
[a] Classification of the corresponding complex (see text for explanations).

occupancies ranging from 0.5:0.5 to 0.7:0.3. The position of highest occupancy was retained for **1f**, **1g** and **1j** and is in agreement with **1e**. For **1d**, **1i**, **1h** and **1k**, for each of which the two positions were equally occupied, we selected that in agreement with **1e**, and for **1l** the oxygen was added manually to bring it into line with other compounds.

After their separation from α-CD, the ligands were named as follows: hydroquinone (**2**), 4-fluorophenol (**3**), 4-methylphenol (**4**), 4-nitrophenol (**5**), 4-chlorophenol (**6**), 4-bromophenol (**7**), 4-hydroxybenzoic acid (**8**), 4-iodophenol (**9**) and 4-iodoaniline (**10**).

2.2. Conformational analysis

The conformational hypersurface of α-CDs was explored with the Hybrid Monte Carlo (HMC) module implemented in MOE [15]. The effect of solvation was taken into consideration; in practice, a set of electrostatic corrections was calculated with the GB/SA method [15–17] and applied to the MMFF94x force field as implemented in MOE.

The conformer with the lowest energy resulting from the conformational analysis (**1c**) was the third conformation of α-CD (besides **1a** and **1b**, see above) stored for calculations (Table 1).

2.3. Geometrical descriptors

For each α-CD conformation, three centroids (Fig. 1C) were defined as dummy atoms using MOE: the first (named P) was due to the 6 oxygen atoms of the primary face, the second (C) to the 6 glycosidic oxygen atoms, and the third (S) to the 12 oxygen atoms of the secondary face. The distances PS, PC and SC were then monitored for all the α-CDs (Table 1).

For each complex, the centroid of the aromatic portion of the ligand was also defined (L) and its distance from the centroid S (see above) was monitored and named SL (Table 1).

2.4. Molecular Interaction Fields (MIFs)

MIFs were calculated using the program GRID [18]. Two probes were chosen for this study, water (OH2) and the hydrophobic probe (DRY). Default parameters were utilized, except for the number of planes of grid points per Angstrom (NPLA directive) which was set to 2.

Since the volume of MIFs varies with the energy cutoff value, −5.0 kcal/mol was taken as cutoff for the hydrophilic field and −0.05 kcal/mol for the hydrophobic field. The MIFs were then exported using readable format and submitted to an in-house program to obtain some numerical descriptors, as described elsewhere [19]. Briefly, our program counts the number of points (known as final points) with energy equal to or below a selected energy cutoff value. The number of points is proportional to the volume of the interaction region and can thus be used as a numerical descriptor. For improved visualization of the results in MOE, final points that are close together in the original grid are joined together to form cubes; a cluster is assumed to form when at the least two cubes have a common side.

All calculations were performed on a Linux based dual-processor Appro1124 server and on standard PCs operating with Microsoft Windows XP.

3. Results and discussion

3.1. Preliminary analysis of the α-CD retrieved from the CSD database

The distances PS, PC and SC (see Fig. 1C) were calculated for all 36 α-CDs retrieved from the CSD (see Section 2.1). In Fig. 2 we ordered the 36 compounds by increasing value of SC and, if available, we reported the log *K* values of the 1:1 complex. Interestingly, low log *K*s (<2) correspond to low SC values (<2) and high log *K*s (>2) correspond to high SC values (>2). This trend suggests that SC might be a geometrical descriptor of interest, and should be investigated in more detail (see Section 3.4).

Fig. 2 shows in white the five α-CDs as such, retrieved from the CSD (see Section 2.1): these have different SC values as would reasonably be expected due to the different experimental conditions used to obtain crystals. After critical data analysis, we selected the α-CD obtained from CHXAMH02 as the reference for use in this study.

3.2. α-CD

The first step of the study consisted in determining the differences between the X-ray structure and the relevant conformations for α-CD obtained by minimization and conformational analysis [19].

Three conformations were considered: (a) the crystallographic structure of α-CD alone without minimization (**1a**), (b) the crystallographic structure of α-CD alone after minimization under MMFF94x and GB-SA conditions (to take the solvent into account) (**1b**) and (c) the lowest energy

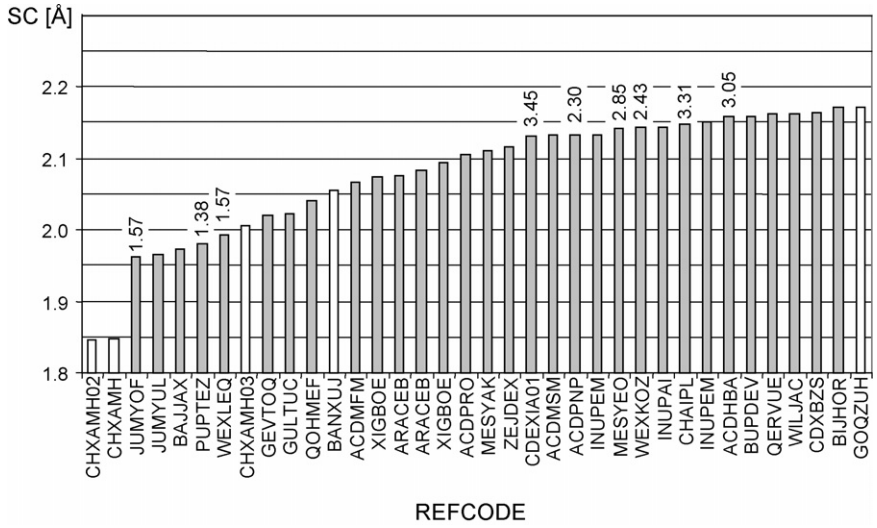

Fig. 2. Values of SC (Å) for the 36 hits retrieved from the CSD (see text for details) and identified by their refcode. Data for α-CD alone (not involved in the formation of inclusion complexes) are in white. Log *K* values for 1:1 inclusion complexes are also reported where available.

conformer resulting from a conformational analysis (**1c**) performed by an HMC simulation (the method used is similar to one of those cited by Lipkowitz [20]).

The crystal packing forces could be responsible for the main differences in geometrical descriptors observed between experimental (**1a**) and calculated (**1b** and **1c**) structures (Table 1).

MIFs were used to study the hydrophobic and hydrophilic content of α-CD conformations separately. Two MIFs were used: the hydrophilic field generated by the OH2 probe and the hydrophobic field generated by the DRY probe [21]. The same energy cutoff values were adopted (−5.0 kcal/mol for the hydrophilic field and −0.05 kcal/mol for the hydrophobic field) and the same colour code (blue for the hydrophilic field and yellow for the hydrophobic field). The balance between the hydrophobic and the polar regions was evaluated from the ratio between the number of final dry points and the number of final water points (r(DRY/OH2)) (Table 2). The higher this ratio, the larger the extension of the hydrophobic regions.

Table 2
MIF numerical results for α-CD in its different conformations (see text)

No.	OH2 (−5 kcal/mol)		DRY (−0.05 kcal/mol)		r(DRY/OH2)[a]
	Final points	Cubes	Final points	Cubes	
1a	1534	72	9	0	0.006
1b	1611	92	78	0	0.055
1c	1604	174	110	1	0.070
1d	1641	75	77	4	0.047
1e	1702	67	88	4	0.052
1f	1675	74	90	6	0.054
1g	1572	86	99	5	0.126
1h	1683	86	278	58	0.165
1i	1702	89	274	60	0.161
1j	1500	59	294	74	0.196
1k	1573	64	290	68	0.184
1l	1584	71	304	70	0.192

Calculations were performed on α-CD as such (=without any ligand).
[a] Ratio between number of dry points and number of water points.

MIFs analysis was both graphic and numerical (Fig. 3, Table 2). A visual inspection of MIFs for **1a** (Fig. 3) showed that blue regions (hydrophilic) were widely dispersed inside the cavity [22] and also around the hydroxyl moieties, whereas yellow regions (hydrophobic) were almost lacking (points are spread and thus cubes cannot form, Table 2). Similar patterns were found for **1b** and **1c**, for which the larger number of yellow points occurred in the outermost regions, of little interest. Interestingly, these results are very similar to those reported for α-CD [19] and confirms the limited hydrophobic nature of the CD cavity [23].

The numerical analysis concerns the variation of r(DRY/OH2) (the ratio between number of dry points and number of water points). At first sight, the variation in r(DRY/OH2) between the three conformers might seem large (Table 2). Indeed, the graphical analysis discussed above, together with the data already obtained for α-CDs [19] suggests that r(DRY/OH2) values below 0.1 may be considered similar, at least in regard to CD molecules.

The limited variability of the hydrophobic/hydrophilic profile among conformations of α-CD not involved in complex formation was confirmed by MIFs data calculated for all the conformers obtained from the HMC simulation (data not shown).

3.3. Type 1 and Type 2 inclusion complexes: definitions and relations with the complex stability constant (log K)

It was only possible to find reliable log *K* values for 10 of the 31 complexes found in the CSD (see Section 3.1). Since 9 out of 10 show an aromatic portion, we decided to eliminate the complex with acetonitrile (code GEVTOQ) from further studies, to make the series more uniform.

In the attempt to find molecular descriptors correlated with log *K*, we first focused on traditional lipophilicity descriptors, since a linear dependence between log *K* and lipophilicity has sometimes been reported [11]. Table 3 shows the lipophilicities of the ligands **2**–**10** (expressed as CLOGP) together with

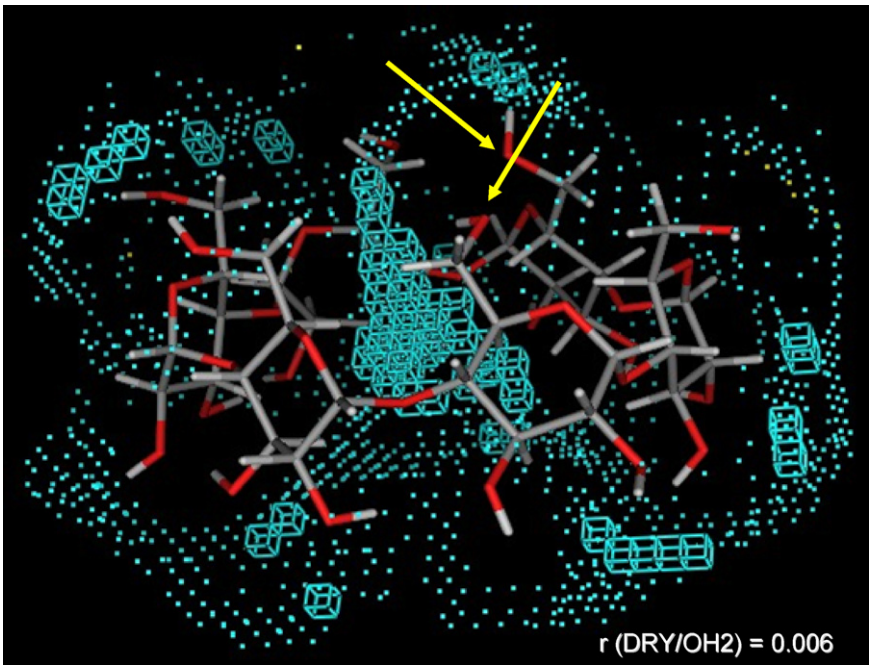

Fig. 3. MIF visualization for α-CD as downloaded from the CSD: hydrophilic regions (blue) at −5.0 kcal/mol and hydrophobic regions (yellow) at −0.05 kcal/mol. The orientation is such that the 2-OH/3-OH side points downward (larger opening of the torus) and the 6-CH_2OH points upwards (smaller opening of the torus). The yellow arrows indicate the oxygens pointing towards the interior of the cavity. The r(DRY/OH2) is also shown.

stability constants (log *K*) of the 1:1 complex. The lowest value (1.38) was recorded for the α-CD complex with hydroquinone, whereas the highest (3.45) was for the complex with 4-iodoaniline. Ligands **2**–**10** are lipophilic (log $P > 0$) and cover a range of about 2.0 logarithm units. For this dataset no relationship ($r^2 < 0.4$) was found between log *K* and CLOGP.

During the course of the present study, a paper by Muraoka et al. [10] came to our attention; starting from an analysis of crystal structures, the group found that α-CD inclusion complexes with *para*-substituted benzenes can be classified into two groups: Type 1 and Type 2. Ligands that enter deeply into the cavity generate Type 1 complexes, whereas those that only enter shallowly into the cavity generate Type 2 complexes. After reading this paper we realized that: (a) Type 1 and Type 2 complexes can likely be related to log *K* values and (b) this classification could be extended to all 1:1 inclusion complexes, provided that some general numerical criteria be given to unambiguously assign complexes to one of the two classes.

Table 3
Virtual log *P* and log *K* values of the investigated ligands

No.	Compound	Log $K_{1:1}$[a]	CLOGP[b]
2	Hydroquinone	1.38	0.81
3	4-Fluorophenol	1.57	1.91
4	4-Methylphenol	1.57	1.97
5	4-Nitrophenol	2.30	1.85
6	4-Chlorophenol	2.43	2.48
7	4-Bromophenol	2.85	2.63
8	4-Hydroxybenzoic acid	3.05[c]	1.56
9	4-Iodophenol	3.31	2.89
10	4-Iodoaniline	3.45	2.32

[a] Taken from the review by Rekharsky and Inoue [12].
[b] CLOGP values.
[c] Taken from the paper by Connors et al. [24].

In an attempt to find criteria to discriminate between Types 1 and 2 complexes, we examined the distances (SL) between the centroid of the secondary oxygens (S) and the centroid of the aromatic ring (L) of the ligands, as reported in Table 1 (see Section 2.3 for definitions). In the presence of positive SL values (once the position of S is fixed, we call those distances that point toward the interior of the cavity positive and those that point outwards negative) we assume that the complex is of Type 1 (Fig. 4A shows α-CD (**1k**) with 4-iodophenol (**9**) as an example), whereas for negative SL values the complex is assumed to be of Type 2 (Fig. 4B shows α-CD (**1e**) with 4-fluorophenol (**3**) as an example). According to this assumption the complexes of α-CD with ligands **2**–**4** are of Type 2, while those with **5**–**10** are of Type 1. Interestingly log *K* values (Table 3) split the complexes into two families corresponding to Type 1 and Type 2: complexes with ligands **2**–**4** have low log *K* values (<2), whereas complexes with ligands **5**–**10** have high log *K* values (>2).

This finding demonstrates the relation between log *K* and the classification of complexes into Types 1 and 2, as obtained by a geometrical descriptor such as SL, but also outlines the limits of using the distance SL as a criterion to distinguish the two classes, since SL depends on the chemical structure of the ligand, and thus cannot be considered for general application.

The orientation of ligands in the CD cavity also seems to vary with the type of complex. To a first approximation, in Type 1 complexes all the phenols (**5**–**9**) have the same orientation, with the hydroxyl group in the region of the secondary hydroxyls; this is the common behavior observed for phenols and anilines (**10** behaves like **9**) [11]. In Type 2 complexes there

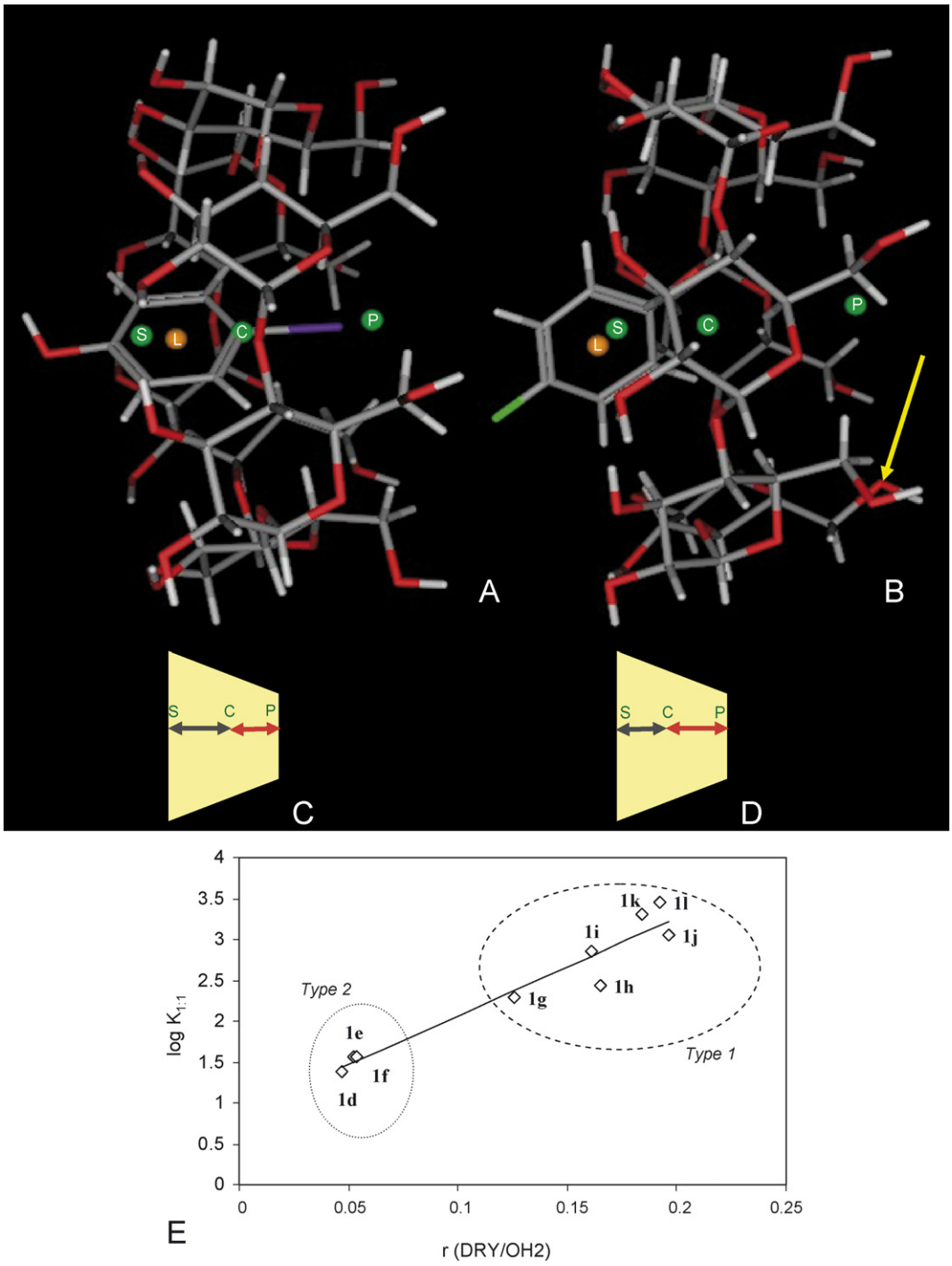

Fig. 4. Classification of inclusion complexes into Type 1 and Type 2. (A) 3D structures of 4-iodophenol complex (Type 1). CD centroids (P, C, and S) are represented by green spots whereas the ligand centroid L is in orange. (B) 3D structures of 4-fluorophenol complex (Type 2). The yellow arrow indicates the oxygen pointing towards the interior of the cavity. (C) Schematic representation of Type 1 complexes. S, C and P are the centroids discussed in the text. The distance SC is larger than CP. (D) Schematic representation of Type 2 complexes. The distance SC is shorter than CP. (E) The plot of the experimental stability complex constant (log $K_{1:1}$) *vs.* the MIF derived descriptor (r(DRY/OH2)). The linear regression line is shown (Eq. (1)).

is no clear evidence about the orientation of ligands: **3** shows the OH group entering the CD cavity, whereas **4** has the methyl group in that position and the OH outside the cavity.

Taken together, the results obtained so far suggest that a general method to distinguish Type 1 from Type 2 complexes must be looked for in an analysis of the CD as such, and not of the whole complex.

3.4. α-CD analysis to distinguish between Type1/Type 2 inclusion complexes

Conformational modifications are proof of the induced fit between host and ligand. Given that this is the case, we hypothesized that variations in α-cyclodextrin structure, and in the related molecular properties caused by the formation of

inclusion complexes, should provide a basis on which to classify the complexes as Type 1 and Type 2. To prove this hypothesis we used both geometrical (SC, see Fig. 1C) and physicochemical (r(DRY/OH2), obtained by the MIFs analysis, see Section 2.4 for definition) descriptors.

The crystallographic structures of the α-CDs alone, after their separation from the ligands were analyzed without further minimization. Clearly this approach gives no information about the mechanisms governing the formation of complexes, and thus an additional study is underway to apply molecular dynamics to CDs systems, in line with other studies [17].

Table 1 shows some geometrical descriptors of **1d**–**1l** (see Fig. 1C for their visualization). The in-depth analysis (see Section 3.1) of their significance is given below.

At first sight one could argue that **1g**–**1l** are more similar to **1a**, the α-CD without any ligand in its crystallographic form, than are **1d**–**1f**, because of the very similar PS values. However, a closer inspection of the data highlights that, for **1g**–**1l**, PS, which reflects PC and SC values, is numerically similar to PS for **1a**, although it is the result of two opposing effects (smaller PC and higher SC). Conversely, the slightly higher PS values for **1d**–**1f** than for **1a** are due to slight changes in PC and SC, both in the same direction. From this evidence, it is reasonable to assume that α-CD takes on two different conformations when employed in the formation of complexes: the first, very similar to that in the absence of any ligand (Fig. 4D), concerns Type 2 complexes, and the second, less similar to the parent, concerns Type 1 complexes (Fig. 4C). This finding points up that, as expected, the influence of the ligands present in Type 2 complexes on the geometry of α-CD is very small compared to that observed for Type 1 complexes.

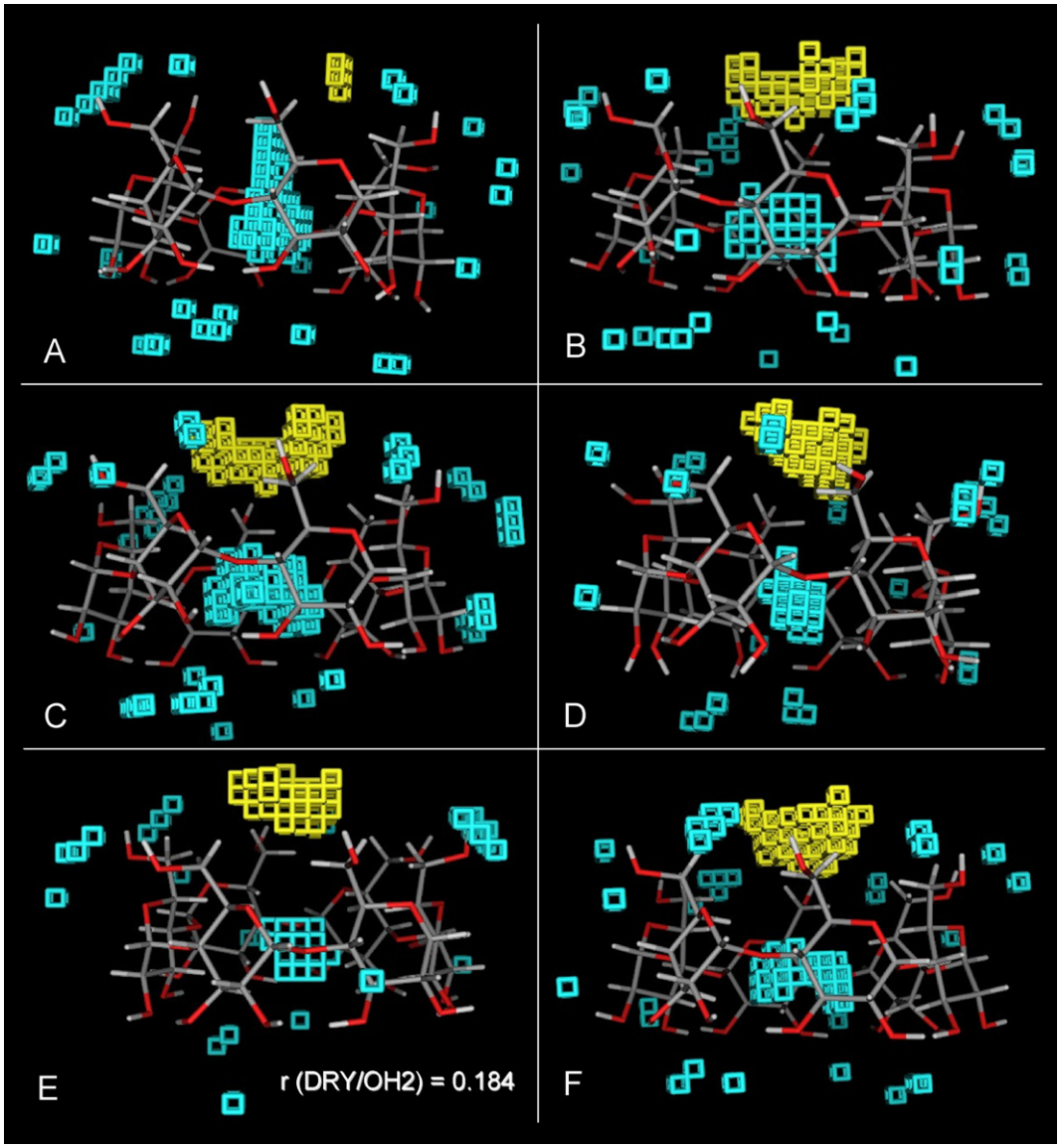

Fig. 5. MIF visualization for Type 1 complexes: cubes resulting from the analysis of MIFs obtained at −5.0 kcal/mol with the OH2 probe (blue) and −0.05 kcal/mol for the DRY probe (yellow). (A) α-CD alone after separation from 4-nitrophenol. (B) α-CD alone after separation from 4-chlorophenol. (C) α-CD alone after separation from 4-bromophenol. (D) α-CD alone after separation from 4-hydroxybenzoic acid. (E) α-CD alone after separation from 4-iodophenol. The r(DRY/OH2) is also shown. (F) α-CD alone after separation from 4-iodoaniline.

MIFs data for α-CDs are in Table 2. The mathematical relationship between log $K_{1:1}$ and r(DRY/OH2) is in Eq. (1) and the corresponding plot is in Fig. 4E:

$$\log K_{1:1} = 12.00(\pm 1.26) \times \mathrm{r(DRY/OH2)} + 0.86(\pm 0.18);$$
$$n = 9,\ \ r^2 = 0.93,\ \ s = 0.23, \qquad (1)$$

where 95% confidence limits are given in parentheses; n is the number of compounds, r^2 the squared correlation coefficient and s is the standard error of the prediction. Interestingly, Fig. 4E shows a correspondence between data calculated for α-CD as such (after separation from the ligand) and the classification of these complexes into Types 1 and 2, since r(DRY/OH2) for Type 2 complexes was not significantly different from the corresponding value recorded for α-CD as such (see Section 3.1) and Type 2 complexes are closely packed into the bottom left-hand corner of the plot. The reverse is true for Type 1 complexes, as is shown in Fig. 4E. Summing up, since Type 2 complexes have a log K values below 2, whereas Type 1 have them above 2, it is possible to take 2 as the threshold value of log K for a first discrimination between Type 1 and Type 2 complexes. The low number of compounds examined suggests caution should be used in calculating log $K_{1:1}$ from Eq. (1), which however is a result of great interest, since it demonstrates the possibility of an *in silico* estimation of log K from the 3D structure of α-CD, which can be obtained from X-ray data, but also from reliable models obtained from computational tools.

Graphic analysis of MIFs gives insight into the location of the hydrophobic regions, whose extension was larger for α-CD as such (after separation from the ligand) for Type 1 complexes (Fig. 5A–F) than for Type 2 complexes (not shown). The hydrophobic zone of α-CD as such for Type 1 complexes is located in the zone of the primary face around the cavity. This behavior is probably due to the deeper entry of the ligands (compared to Type 2 ligands), which causes the primary oxygens to open [19].

This result indicates that it would be reasonable to consider as ''true'' inclusion complexes only those of Type 1, since for those of Type 2 the presence of the ligand does not significantly alter the polar/hydrophobic pattern of α-CD from that of the parent. This assumption is supported by the observation of an oxygen pointing toward the interior of the cavity (yellow arrow in Fig. 4B). It was verified (data not shown) that such an orientation for a primary oxygen can only occur for α-CDs involved in Type 2 complexes, since inclusion of the ligand is only partial and does not greatly affect the geometry of α-CD, which originally bears two oxygens pointing towards the interior of the cavity (see Fig. 3).

3.5. The complex of 4-iodophenol with α-CD as an example of Type 1 complex

Since similar behavior occurred for the six Type 1 complexes (see Section 3.4), we analyzed the MIF results in greater depth, using the complex of 4-iodophenol with α-CD as a representative example.

Fig. 6 shows the MIF pattern of 4-iodophenol (Fig. 6A) and that of its complex with α-CD (Fig. 6B). Note that the calculation, whose results are given in Fig. 6B, is the only one that was performed on the complex as a whole, and not on the α-CD molecule alone. These two images should be compared with that in Fig. 5E which, as was said above, represents the corresponding profile for the α-CD alone, resulting after its separation from the ligand, and with that in Fig. 3, which shows the crystallographic structure of α-CD as such. The MIF results highlight that the almost completely hydrophilic α-CD in Fig. 3 (r(DRY/OH2) = 0.006) is able to incorporate the very lipophilic ligand in Fig. 6A (r(DRY/OH2) = 244.10) with significant but localized modification of its polar/hydrophilic pattern (Fig. 5E,

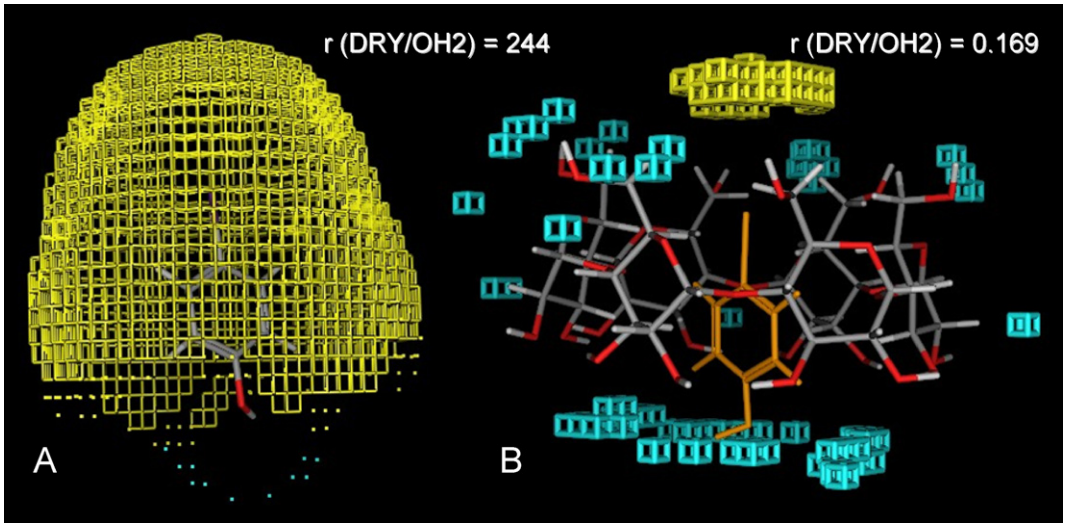

Fig. 6. MIF visualization resulting from the analysis of MIFs obtained at −5.0 kcal/mol with the OH2 probe (blue) and −0.05 kcal/mol for the DRY probe (yellow). The r(DRY/OH2) values are also shown. (A) 4-Iodophenol: cubes and points are represented; (B) complex of α-CD with 4-iodophenol (in orange): only cubes are represented.

r(DRY/OH2) = 0.184). The resulting complex (Fig. 6B) maintains the profile of the α-CD (r(DRY/OH2) = 0.169) from the numerical standpoint, but shows a displacement of the polar region from the interior of the cavity to the area surrounding the secondary face.

This shows that α-CD can mask the undesirable high lipophilicity (often linked to poor aqueous solubility) of ligands by slightly altering its own polar/hydrophobic pattern, this in turn being responsible for the favorable pharmacokinetic profile of the complex.

Finally, it should be pointed out that this paper focuses on complexes that are formed by ligands of small size able to enter almost completely into the cavity. Work is in progress to extend the study to include larger ligands, in order to analyze the significance of the ligand portion that remains outside the cavity.

4. Conclusions

The computational prediction of log K is an important task in medicinal chemistry and pharmaceutical sciences, because of the significance of host-guest systems in improving drug bioavailability. We here define *in silico* descriptors (one geometrical and one physicochemical) enabling Type 2 complexes (with log $K < 2$) to be separated from Type 1 complexes (with log $K > 2$) formed by α-CD. The method is based on analysis of the α-CD structures (X-ray data but 3D models of good reliability obtained from computational tools, are expected to give the same results) and thus is of general application, since it avoids the limitations due to the chemical structure of the ligand.

Since the results presented here show that α-CD behaves similarly to α-CD, a study is underway to extend the work to include γ-CDs and to derivatised CDs belonging to the various CD families.

Acknowledgement

GE and GC are indebted to the University of Turin for financial support.

References

[1] H. van de Waterbeemd, D.A. Smith, K. Beaumont, D.K. Walker, Property-based design: optimization of drug absorption and pharmacokinetics, J. Med. Chem. 44 (2001) 1313–1333.
[2] M.E. Davis, M.E. Brewster, Cyclodextrin-based pharmaceutics: past, present and future, Nat. Rev. Drug Discov. 3 (2004) 1023–1035.
[3] G.L. Amidon, H. Lennernaes, V.P. Shah, J.R. Crison, A theoretical basis for a biopharmaceutic drug classification: the correlation of in vitro drug product dissolution and in vivo bioavailability, Pharm. Res. 12 (1995) 413–420.
[4] N.A. Kasim, M. Whitehouse, C. Ramachandran, M. Bermejo, H. Lennernaes, A.S. Hussain, H.E. Junginger, S.A. Stavehansky, K.K. Midha, V.P. Shah, G.L. Amidon, Molecular properties of WHO essential drugs and provisional biopharmaceutical classification, Mol. Pharm. 1 (2004) 85–96.
[5] D.O. Thompson, Cyclodextrins-enabling excipients: their present and future use in pharmaceuticals, Crit. Rev. Ther. Drug Carrier Syst. 14 (1997) 1–104.
[6] J. Szejtli, Introduction and general overview of cyclodextrin chemistry, Chem. Rev. 98 (1998) 1743–1753.
[7] V.J. Stella, R.A. Rajewski, Cyclodextrins: their future in drug formulation and delivery, Pharm. Res. 14 (1997) 556–567.
[8] S. Baboota, R. Khanna, S.P. Agarwal, J. Ali, A. Ahuja, Cyclodextrins in drug delivery systems: an update, Pharma Articles.NET, 2003.
[9] F.W. Lichtenthaler, S. Immel, On the hydrophobic characteristics of cyclodextrins: computer-aided visualization of molecular lipophilicity patterns, Liebigs Ann. (1996) 27–37.
[10] S. Muraoka, O. Matsuzaka, S. Kamitori, K. Okuyama, Crystal structures of cyclomaltohexaose (α-cyclodextrin) complexes with *p*-chlorophenol and *p*-cresol, Carbohydr. Res. (1999) 261–266.
[11] K.A. Connors, The stability of cyclodextrin complexes in solution, Chem. Rev. 97 (1997) 1325–1357.
[12] M.V. Rekharsky, Y. Inoue, Complexation thermodynamics of cyclodextrins, Chem. Rev. 98 (1998) 1875–1917.
[13] Mercury, Version 1.3, CCDC, Cambridge, UK, 2005 http://www.ccdc.cam.ac.uk/products/csd_system/mercury/.
[14] MOE, Version 2005.06, Chemical Computing Group, Montreal, Quebec, Canada, 2005 http://www.chemcomp.com/.
[15] G. Caron, G. Ermondi, A. Damiano, L. Novaroli, O. Tsinman, J.A. Ruell, A. Avdeef, Ionization, lipophilicity, and molecular modeling to investigate permeability and other biological properties of amlodipine, Bioorg. Med. Chem. 12 (2004) 6107–6118.
[16] D. Qiu, P.S. Shenkin, F.P. Hollinger, W.C. Still, The GB/SA continuum model for solvation. A fast analytical method for the calculation of approximate born radii, J. Phys. Chem. A 101 (1997) 3005–3014.
[17] G. Uccello-Barretta, F. Balzano, D. Paolino, R. Ciaccio, S. Guccione, Combined NMR-crystallographic and modelling investigation of the inclusion of molsidomine into α-, β-, and γ-cyclodextrins, Bioorg. Med. Chem. 13 (2005) 6502–6512.
[18] GRID, Version 22b, Molecular Discovery Ltd., West Way House, Elms Parade, Oxford, 2004 http://www.moldiscovery.com.
[19] G. Ermondi, C. Anghilante, G. Caron, A combined *in silico* strategy to describe the variation of some 3D molecular properties of β-cyclodextrin due to the formation of inclusion complexes, J. Mol. Graph. Model. 25 (2006) 296–303.
[20] K.B. Lipkowitz, Applications of computational chemistry to the study of cyclodextrin, Chem. Rev. 98 (1998) 1829–1873.
[21] G. Cruciani, P. Crivori, P.A. Carrupt, B. Testa, Molecular fields in quantitative structure-permeation relationships: the VolSurf approach, J. Mol. Struct. (Theochem.) 503 (2000) 17–30.
[22] G. Uccello-Barretta, F. Balzano, G. Sicoli, C. Friglola, I. Aldana, A. Monge, D. Paolino, S. Guccione, Combining NMR and molecular modelling in a drug delivery context: investigation of the multi-mode inclusion of a new NPY-5 antagonist bromobenzenesulfonamide into β-cyclodextrin, Bioorg. Med. Chem. 12 (2004) 447–458.
[23] F.W. Lichtenthaler, S. Immel, Towards understanding formation and stability of cyclodextrin inclusion complexes: computation and visualization of their molecular lipophilicity patterns, Starch/Stärke 48 (1996) 145–154.
[24] K.A. Connors, S.-F. Lin, A. Wong, Potentiometric study of molecular complexes of weak acids and bases applied to complexes of α-cyclodextrin with *para*-substituted benzoic acids, J. Pharm. Sci. 71 (1982) 217–222.